

DGFEM FOR INTERACTION OF FLUIDS AND NONLINEAR ELASTICITY

MILOSLAV FEISTAUER*, MARTIN HADRAVA†, ADAM KOŠÍK‡, AND JAROMÍR HORÁČEK§

Abstract. This paper is concerned with the numerical simulation of the interaction of compressible viscous flow with elastic structures. The flow is described by the compressible Navier-Stokes equations written in the arbitrary Lagrangian-Eulerian (ALE) form. For the elastic deformation we use 2D linear elasticity and nonlinear St. Venant-Kirchhoff and neo-Hookean models. The discretization of both flow problem and elasticity problem is realized by the discontinuous Galerkin finite element method (DGFEM). The main attention is paid to testing the DGFEM applied to the solution of elasticity problems. Then we present an example of the fluid-structure interaction (FSI). The applicability of the developed technique is demonstrated by several numerical experiments.

Key words. compressible Navier-Stokes equations, ALE method, nonlinear dynamic elasticity, discontinuous Galerkin method, fluid-structure interaction

AMS subject classifications. 65M60, 74H15, 76M10

1. Introduction. The study of flow-induced vibrations of elastic structures plays an important role in a number of fields in science and technology. We can mention, e.g., vibrations of airplane wings or turbine blades, interaction of wind with bridges, TV towers or cooling towers of power stations. This subject also becomes more and more relevant in biomechanics, e.g., in the simulation of blood flow in veins and heart or the analysis the vocal folds vibrations induced by air flowing from lungs. The goal of our research is the numerical simulation of interaction of compressible 2D viscous flow in the glottal region with a compliant tissue of the human vocal folds modeled by a 2D elastic structure. The primary voice source is given by the airflow coming from the lungs that causes self-oscillations of the vocal folds ([6]). The simulation of these processes contains two main ingredients: the solution of flow problem in a time dependent domain and the solution of the deformation of an elastic body. In our paper, the main attention is paid to the numerical solution of dynamic linear and nonlinear elasticity problems. The space discretization is carried out by the discontinuous Galerkin finite element method (DGFEM) based on the piecewise linear approximation of the sought solution without any requirement of the continuity on interfaces between neighbouring elements (see, e.g., [3]). For the time discretization the backward difference formula (BDF) method is used. Two models of nonlinear material are considered: St. Venant-Kirchhoff model and neo-Hookean model. The numerical method is tested with the aid of numerical experiments using the benchmark proposed by J. Hron and S. Turek in [7].

*Charles University in Prague, Faculty of Mathematics and Physics, Sokolovská 83, 186 75 Praha 8, Czech Republic (feist@karlin.mff.cuni.cz).

†Charles University in Prague, Faculty of Mathematics and Physics, Sokolovská 83, 186 75 Praha 8, Czech Republic (martin@hadrava.eu).

‡Charles University in Prague, Faculty of Mathematics and Physics, Sokolovská 83, 186 75 Praha 8, Czech Republic and University of Dortmund, LS III, Vogelpothsweg 87, 44277 Dortmund, Germany (adam.kosik.cz@gmail.com).

§Institute of Thermomechanics, The Academy of Sciences of the Czech Republic, v. v. i., Dolejškova 1402/5, 182 00 Praha 8, Czech Republic (jaromirh@it.cas.cz).

Then the developed numerical schemes are applied together with the discontinuous Galerkin method for the solution of compressible flow ([1], [3]) to the simulation of vocal folds vibrations induced by air flow.

2. Description of the dynamic elasticity problem. Let us consider an elastic body represented by a bounded domain $\Omega^b \subset \mathbb{R}^2$ with Lipschitz boundary $\partial\Omega^b$. We assume that the boundary of the domain Ω^b consists of two disjoint parts, namely a Dirichlet part Γ_D^b and a Neumann part Γ_N^b . The deformation of the body is described by the displacement $\mathbf{u} : \Omega^b \times [0, T] \rightarrow \mathbb{R}^2$ and the deformation mapping $\varphi(\mathbf{X}, t) = \mathbf{X} + \mathbf{u}(\mathbf{X}, t)$, $\mathbf{X} \in \Omega^b$, $t \in [0, T]$, where $[0, T]$ with $T > 0$ is a time interval. Further, we introduce the following notation: deformation gradient $\mathbf{F} = \nabla\varphi$, the Jacobian $J = \det \mathbf{F} > 0$ and the Green strain tensor $\mathbf{E} \in \mathbb{R}^{2 \times 2}$:

$$(2.1) \quad \mathbf{E} = \frac{1}{2} \left(\mathbf{F}^T \mathbf{F} - \mathbf{I} \right), \quad \mathbf{E} = (E_{ij})_{i,j=1}^2.$$

with components

$$(2.2) \quad E_{ij} = \frac{1}{2} \left(\frac{\partial u_i}{\partial X_j} + \frac{\partial u_j}{\partial X_i} \right) + \frac{1}{2} \sum_{k=1}^2 \frac{\partial u_k}{\partial X_i} \frac{\partial u_k}{\partial X_j}.$$

We set $\text{tr}(\mathbf{E}) = \sum_{i=1}^2 E_{ii}$ and by \mathbf{I} we denote the unit tensor, represented by the unit matrix. Further, we introduce the first Piola-Kirchhoff stress tensor \mathbf{P} . Its form depends on the chosen elasticity model.

Now we formulate the general dynamic elasticity problem. We want to find a displacement function $\mathbf{u} : \Omega^b \times [0, T] \rightarrow \mathbb{R}^2$ such that

$$(2.3) \quad \rho^b \frac{\partial^2 \mathbf{u}}{\partial t^2} + C_M \rho^b \frac{\partial \mathbf{u}}{\partial t} - \text{div} \mathbf{P} = \mathbf{f} \quad \text{in } \Omega^b \times [0, T],$$

$$(2.4) \quad \mathbf{u} = \mathbf{u}_D \quad \text{in } \Gamma_D^b \times [0, T],$$

$$(2.5) \quad \mathbf{P} \cdot \mathbf{n} = \mathbf{g}_N \quad \text{in } \Gamma_N^b \times [0, T],$$

$$(2.6) \quad \mathbf{u}(\cdot, 0) = \mathbf{u}_0, \quad \frac{\partial \mathbf{u}}{\partial t}(\cdot, 0) = \mathbf{z}_0 \quad \text{in } \Omega^b,$$

where $\mathbf{f} : \Omega^b \times [0, T] \rightarrow \mathbb{R}^2$ is the density of the acting body force, $\mathbf{g}_N : \Gamma_N^b \times [0, T] \rightarrow \mathbb{R}^2$ is the surface traction acting on the Neumann part of the boundary Γ_N^b , $\mathbf{u}_D : \Gamma_D^b \times [0, T] \rightarrow \mathbb{R}^2$ is the prescribed displacement on the Dirichlet part of the boundary Γ_D^b , $\mathbf{u}_0 : \Omega^b \rightarrow \mathbb{R}^2$ is the initial displacement, $\mathbf{z}_0 : \Omega^b \rightarrow \mathbb{R}^2$ is the initial deformation velocity, $\rho^b > 0$ is the material density and $C_M \geq 0$ is the damping coefficient.

We consider three elasticity models. Cf. [2].

St. Venant-Kirchhoff material. In this case we set

$$(2.7) \quad \mathbf{P} = \mathbf{F} \boldsymbol{\Sigma},$$

where

$$(2.8) \quad \boldsymbol{\Sigma} = \lambda^b \text{tr}(\mathbf{E}) \mathbf{I} + 2\mu^b \mathbf{E},$$

is the second Piola-Kirchhoff stress tensor. The coefficients λ^b and μ^b are the Lamé parameters. They are usually expressed with the aid of the Young modulus E^b and the Poisson ratio ν^b according to the relations

$$(2.9) \quad \lambda^b = \frac{E^b \nu^b}{(1 + \nu^b)(1 - 2\nu^b)}, \quad \mu^b = \frac{E^b}{2(1 + \nu^b)}.$$

Writing $\boldsymbol{\Sigma} = (\Sigma_{ij})_{i,j=1}^2$, we get

$$(2.10) \quad \begin{aligned} \Sigma_{ij} = & \lambda^b \left(\sum_{l=1}^2 \frac{\partial u_l}{\partial X_l} + \frac{1}{2} \sum_{l=1}^2 \sum_{k=1}^2 \left(\frac{\partial u_k}{\partial X_l} \right)^2 \right) \delta_{ij} \\ & + \mu^b \left(\frac{\partial u_i}{\partial X_j} + \frac{\partial u_j}{\partial X_i} + \sum_{k=1}^2 \frac{\partial u_k}{\partial X_i} \frac{\partial u_k}{\partial X_j} \right). \end{aligned}$$

Neo-Hookean material. As another example we consider the neo-Hookean material, for which the first Piola-Kirchhoff stress tensor has the form

$$(2.11) \quad \mathbf{P} = \mu^b (\mathbf{F} - \mathbf{F}^{-T}) + \lambda^b \log(\det \mathbf{F}) \mathbf{F}^{-T}$$

or equivalently,

$$(2.12) \quad \mathbf{P} = \mu^b \mathbf{F} + (\lambda^b \log(\det \mathbf{F}) - \mu^b) \mathbf{F}^{-T} = \mu^b \mathbf{F} + \frac{\lambda^b \log(\det \mathbf{F}) - \mu^b}{\det \mathbf{F}} \text{Cof} \mathbf{F}.$$

Here $\text{Cof} \mathbf{F}$ is the cofactor of the matrix \mathbf{F} defined as $\text{Cof} \mathbf{F} = J \mathbf{F}^{-T}$.

Linear elasticity model is the simplest elasticity model obtained by the assumption of small deformations. By this assumption the second term in (2.2) is neglected and the linear approximation of \mathbf{E} (linear with respect to the gradient \mathbf{F}) is denoted by \mathbf{e} and called the *small strain tensor*. Then $\mathbf{E} = \mathbf{e} = (e_{ij})_{i,j=1}^2$ and

$$(2.13) \quad e_{ij} = \frac{1}{2} \left(\frac{\partial u_i}{\partial X_j} + \frac{\partial u_j}{\partial X_i} \right).$$

In this case we write

$$(2.14) \quad \mathbf{P} = \lambda^b \text{tr}(\mathbf{e}) \mathbf{I} + 2\mu^b \mathbf{e}.$$

As we see, we have $\mathbf{F} = \mathbf{F}(\mathbf{u})$, $\mathbf{E} = \mathbf{E}(\mathbf{u})$, $\boldsymbol{\Sigma} = \boldsymbol{\Sigma}(\mathbf{u})$, $\mathbf{P} = \mathbf{P}(\mathbf{u})$.

Because of the time discretization, we rewrite the dynamic elasticity problem as the following system of first-order in time for the displacement $\mathbf{u} : \Omega^b \times [0, T] \rightarrow \mathbb{R}^2$ and the deformation velocity $\mathbf{z} : \Omega^b \times [0, T] \rightarrow \mathbb{R}^2$:

$$(2.15) \quad \rho^b \frac{\partial \mathbf{z}}{\partial t} + C_M \rho^b \mathbf{z} - \text{div} \mathbf{P} = \mathbf{f}, \quad \frac{\partial \mathbf{u}}{\partial t} - \mathbf{z} = 0 \quad \text{in } \Omega^b \times [0, T],$$

$$(2.16) \quad \mathbf{u} = \mathbf{u}_D \quad \text{in } \Gamma_D^b \times [0, T],$$

$$(2.17) \quad \mathbf{P} \mathbf{n} = \mathbf{g}_N \quad \text{in } \Gamma_N^b \times [0, T],$$

$$(2.18) \quad \mathbf{u}(\cdot, 0) = \mathbf{u}_0, \quad \mathbf{z}(\cdot, 0) = \mathbf{z}_0 \quad \text{in } \Omega^b.$$

3. Discrete problem. The discretization of the dynamic elasticity problem will be carried out by the discontinuous Galerkin finite element method (DGFEM) in space and the backward difference formula (BDF) method in time. In structural mechanics, usually classical conforming finite elements are used. However, dynamic elasticity leads to problems with hyperbolic character and in the case of nonlinear models we can compare it to nonlinear hyperbolic systems of conservation laws. This is the motivation for the application of the DGM in this case, similarly as for compressible flow.

3.1. Notation. By Ω_h^b we denote a polygonal approximation of the domain Ω^b . The sets $\Gamma_{Dh}^b, \Gamma_{Nh}^b \subset \partial\Omega_h^b$ will approximate Γ_D^b and Γ_N^b . Let \mathcal{T}_h^b be a partition of the closure $\overline{\Omega}_h^b$ formed by a finite number of closed triangles with disjoint interiors.

Let us consider a partition of the time interval $[0, T]$ formed by time instants $t_k = k\tau, k = 0, \dots, M$, where M is a sufficiently large positive integer and $\tau = T/M$ is the time step. (For simplicity we consider a constant time step and, hence, a uniform partition of the interval $[0, T]$. The generalization to a nonuniform partition is possible.) We set $I_k = (t_{k-1}, t_k), k = 1, \dots, M$.

Let $p > 0$ be an integer. By S_{hp} we denote the space of piecewise polynomial functions on the triangulation \mathcal{T}_h^b ,

$$(3.1) \quad S_{hp} = \{v \in L^2(\Omega_h^b); v|_K \in P^p(K), K \in \mathcal{T}_h^b\},$$

where $P^p(K)$ denotes the space of polynomial functions of degree $\leq p$ on the element K . The approximate solution will be sought in $\mathcal{S}_{hp} = S_{hp} \times S_{hp}$ at each time level.

By \mathcal{F}_h^b we denote the system of all faces of all elements $K \in \mathcal{T}_h^b$ and $\mathcal{F}_h^{bB}, \mathcal{F}_h^{bD}, \mathcal{F}_h^{bN}$ and \mathcal{F}_h^{bI} will denote the sets of all boundary, Dirichlet, Neumann and inner faces, respectively. We set $\mathcal{F}_h^{bID} = \mathcal{F}_h^{bI} \cup \mathcal{F}_h^{bD}$. Further, for each $\Gamma \in \mathcal{F}_h^{bI}$ there exist two neighbouring elements $K_\Gamma^{(L)}, K_\Gamma^{(R)} \in \mathcal{T}_h^b$ such that $\Gamma \subset \partial K_\Gamma^{(L)} \cap \partial K_\Gamma^{(R)}$. For each $\Gamma \in \mathcal{F}_h^b$ we define a unit normal vector \mathbf{n}_Γ . We assume that for $\Gamma \in \mathcal{F}_h^{bB}$ the normal \mathbf{n}_Γ has the same orientation as the outer normal to $\partial\Omega^b$. We use the convention that \mathbf{n}_Γ is the outer normal to $\partial K_\Gamma^{(L)}$ and the inner normal to $\partial K_\Gamma^{(R)}$. For $\mathbf{v} \in \mathcal{S}_{hp}$ we introduce the following notation: $\mathbf{v}|_\Gamma^{(L)}$ = the trace of $\mathbf{v}|_{K_\Gamma^{(L)}}$ on Γ , $\mathbf{v}|_\Gamma^{(R)}$ = the trace of $\mathbf{v}|_{K_\Gamma^{(R)}}$ on Γ , $\langle \mathbf{v} \rangle_\Gamma = \frac{1}{2} (\mathbf{v}|_\Gamma^{(L)} + \mathbf{v}|_\Gamma^{(R)})$, $[\mathbf{v}]_\Gamma = \mathbf{v}|_\Gamma^{(L)} - \mathbf{v}|_\Gamma^{(R)}$, where $\Gamma \in \mathcal{F}_h^{bI}$. If $\Gamma \in \mathcal{F}_h^{bB}$, then there exists an element $K_\Gamma^{(L)} \in \mathcal{T}_h^b$ such that $\Gamma \subset K_\Gamma^{(L)} \cap \partial\Omega_h^b$ and we set $\mathbf{v}|_\Gamma^{(L)}$ = the trace of $\mathbf{v}|_{K_\Gamma^{(L)}}$ on Γ , $\langle \mathbf{v} \rangle_\Gamma = [\mathbf{v}]_\Gamma = \mathbf{v}|_\Gamma^{(L)}$. Finally, we set $h_\Gamma = (h_{K_\Gamma^{(L)}} + h_{K_\Gamma^{(R)}})/2$.

3.2. DGM forms. In the derivation of the space discretization by the DGFEM the following process is essential. We multiply the governing system by a test function $\mathbf{v} \in \mathcal{S}_{hp}$, integrate the resulting relations over elements $K \in \mathcal{T}_h^b$, apply Green's theorem to the term containing \mathbf{P} , add some mutually vanishing terms, use boundary conditions and sum over all elements. In this way we get the following forms:

$$(3.2) \quad a_h^b(\mathbf{u}, \mathbf{v}) = \sum_{K \in \mathcal{T}_h^b} \int_K \mathbf{P}(\mathbf{u}) : \nabla \mathbf{v} \, d\mathbf{x} - \sum_{\Gamma \in \mathcal{F}_h^{bID}} \int_\Gamma ((\mathbf{P}(\mathbf{u}))\mathbf{n}) \cdot [\mathbf{v}] \, dS,$$

$$(3.3) \quad J_h^b(\mathbf{u}, \mathbf{v}) = \sum_{\Gamma \in \mathcal{F}_h^{bID}} \int_\Gamma \frac{C_W^b}{h_\Gamma} [\mathbf{u}] \cdot [\mathbf{v}] \, dS,$$

$$(3.4) \quad \ell_h^b(\mathbf{v}) = \sum_{K \in \mathcal{T}_h^b} \int_K \mathbf{f} \cdot \mathbf{v} \, d\mathbf{x} + \sum_{\Gamma \in \mathcal{F}_h^{bN}} \int_\Gamma \mathbf{g}_N \cdot \mathbf{v} \, dS + \sum_{\Gamma \in \mathcal{F}_h^{bD}} \int_\Gamma \frac{C_W^b}{h_\Gamma} \mathbf{u}_D \cdot \mathbf{v} \, dS,$$

$$(3.5) \quad A_h^b = a_h^b + J_h^b,$$

$$(3.6) \quad (\mathbf{u}, \mathbf{v})_{\Omega_h^b} = \int_{\Omega_h^b} \mathbf{u} \cdot \mathbf{v} \, d\mathbf{x} = \sum_{K \in \mathcal{T}_h^b} \int_K \mathbf{u} \cdot \mathbf{v} \, d\mathbf{x},$$

where $\mathbf{u}, \mathbf{v} \in \mathcal{S}_{hp}$ and $C_W^b > 0$ is a sufficiently large constant.

3.3. Backward-difference formula method. By \mathbf{u}^k and \mathbf{z}^k we denote the approximate solution at time t_k , $k = 0, \dots, M$, i.e. $\mathbf{u}^k \approx \mathbf{u}(t_k)$, $\mathbf{z}^k \approx \mathbf{z}(t_k)$. A general backward difference formula approximating the time derivative reads

$$(3.7) \quad \frac{\partial \mathbf{u}}{\partial t}(t_{k+1}) \approx \frac{1}{\tau} \sum_{j=0}^l c_l \mathbf{u}^{k+1-j},$$

where l is the order of the method and c_j , $j = 0, \dots, l$, are the coefficients.

The BDF time discretization of system (2.15) reads

$$(3.8) \quad \frac{\rho^b}{\tau} \sum_{j=0}^l c_l \mathbf{z}^{k+1-j} + C_M \rho^b \mathbf{z}^{k+1} - \operatorname{div} \mathbf{P}^{k+1} = \mathbf{f}^{k+1},$$

$$(3.9) \quad \frac{1}{\tau} \sum_{j=0}^l c_l \mathbf{u}^{k+1-j} - \mathbf{z}^{k+1} = 0$$

in Ω_h^b , where $\mathbf{P}^{k+1} = \mathbf{P}(\mathbf{u}^{k+1})$ and $\mathbf{f}^{k+1} = \mathbf{f}(t_{k+1})$.

Now we apply the process described in Section 3.2 to arrive at the following formulation: the BDF-DG approximate solution of problem (2.15)–(2.18) is defined as a couple of sequences $\{\mathbf{u}_h^k\}_{k=0}^M$, $\{\mathbf{z}_h^k\}_{k=0}^M$ such that

$$(3.10) \quad \begin{aligned} \text{a) } & \mathbf{u}_h^k, \mathbf{z}_h^k \in \mathbf{S}_{hp}, \quad k = 0, \dots, M, \\ \text{b) } & \left(\frac{\rho^b}{\tau} \sum_{j=0}^l c_l \mathbf{z}_h^{k+1-j}, \mathbf{v}_h \right)_{\Omega_h^b} + (C_M \rho^b \mathbf{z}_h^{k+1}, \mathbf{v}_h)_{\Omega_h^b} + A_h^b(\mathbf{u}_h^{k+1}, \mathbf{v}_h) \\ & = \ell_h^b(\mathbf{v}_h)(t_{k+1}) \quad \forall \mathbf{v}_h \in \mathbf{S}_{hp}, \\ \text{c) } & \left(\frac{\rho^b}{\tau} \sum_{j=0}^l c_l \mathbf{u}_h^{k+1-j}, \mathbf{v}_h \right)_{\Omega_h^b} - (\mathbf{z}_h^{k+1}, \mathbf{v}_h)_{\Omega_h^b} = 0 \quad \forall \mathbf{v}_h \in \mathbf{S}_{hp}, \\ & k = 0, \dots, M-1, \\ \text{d) } & (\mathbf{u}_h^0 - \mathbf{u}_0, \mathbf{v}_h)_{\Omega_h^b} = 0, \quad (\mathbf{z}_h^0 - \mathbf{z}_0, \mathbf{v}_h)_{\Omega_h^b} = 0 \quad \forall \mathbf{v}_h \in \mathbf{S}_{hp}. \end{aligned}$$

The initial values \mathbf{u}_h^k , \mathbf{z}_h^k , $k = 1, \dots, l$ are obtained by k -step BDF schemes.

In the numerical experiments we use the second order BDF method with $l = 2$ and $c_0 = 3/2$, $c_1 = -2$, $c_2 = 1/2$. In the first step we use the BDF of the first order with $l = 1$, $c_0 = 1$, $c_1 = -1$.

The discrete nonlinear problems are solved on each time level by the Newton method. For the solution of linear subproblems either direct UMFPAK solver or GMRES method with block diagonal preconditioning are used.

4. Dynamic elasticity test problem. The applicability and accuracy of the presented method is tested on the benchmark problem denoted by CSM3 proposed by J. Hron and S. Turek ([7]). We consider a 2D domain represented by a rigid cylinder with an attached elastic beam behind, as see in Fig. 3.1. The circle has radius $r = 0.05$ m and the beam has length $l = 0.35$ m and height $h = 0.02$ m. Further we define a control point A in the middle of the end of the beam as shown in Fig. 3.1. The evolution of the position of the point $A = A(t)$ is the quantity of our

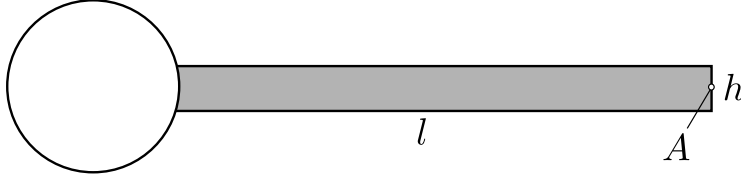


FIG. 3.1. Rigid cylinder with an elastic beam of the nonlinear elasticity benchmark problem.

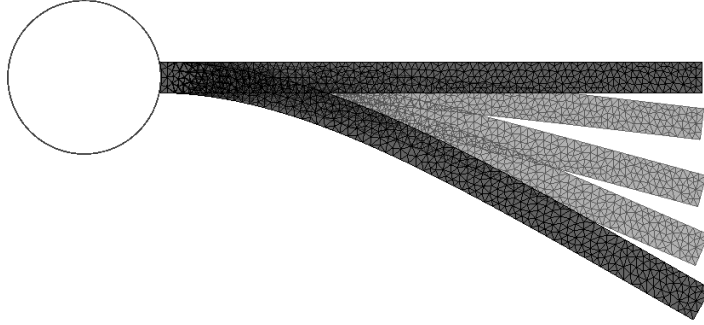


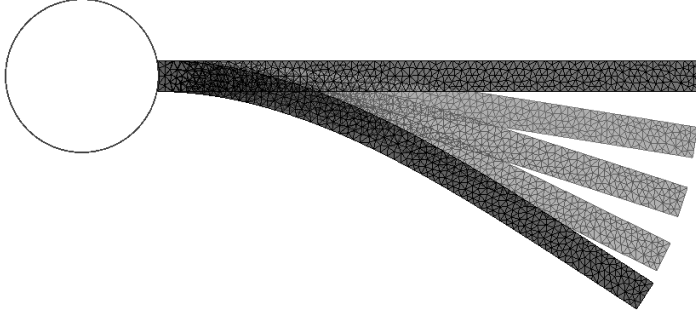
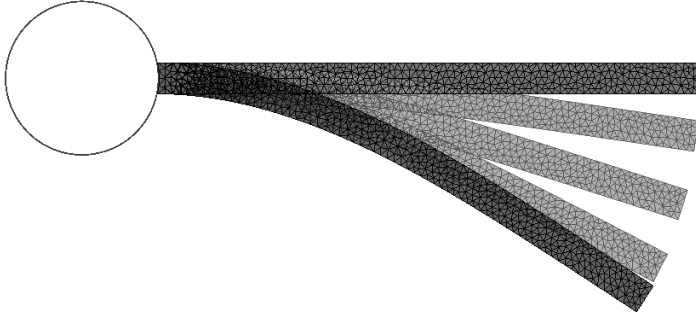
FIG. 3.2. Linear elasticity: The deformation of the beam in case CSM3.

interest. In [7] the elastic beam is modelled as the St. Venant-Kirchhoff material. In addition, here we consider also neo-Hookean material and the linear elasticity model.

The following data are used: $\mathbf{f} = (0, -2\rho^b)^T$ [m.s⁻²], $\rho^b = 10^3$ [kg.m⁻³], on the left part Γ_D^b of the boundary connected with the rigid body we prescribe homogeneous Dirichlet boundary condition $\mathbf{u}_D = \mathbf{0}$ and on the rest part Γ_N^b of the boundary we prescribe the Neumann boundary condition with no surface traction $\mathbf{g}_N = \mathbf{0}$. The initial conditions $\mathbf{u}_0 = \mathbf{z}_0 = \mathbf{0}$. The material is characterized by the Young modulus $E^b = 1.4 \cdot 10^6$ and the Poisson ratio $\nu^b = 0.4$.

Figures 3.2, 3.3, and 3.4 demonstrate the deformation of the beam at several time instants computed by the linear model, St. Venant-Kirchhoff and neo-Hookean model, respectively. There is no significant difference between both nonlinear models in contrast to the linear model, which does not give results correct from the physical point of view.

In the following tables we present the comparison between the reference results of the CSM3 benchmark with our computation carried out by the second-order BDF2 time discretization with several time steps and polynomial degrees in the space discretization. According to [7], the time dependent values are represented by the mean value, amplitude and frequency. The mean value and amplitude are computed from the last period of the oscillations by taking the maximum (max) and minimum (min) values. Then mean = $1/2(\max + \min)$, and amplitude = $1/2(\max - \min)$. The frequency of the oscillations is computed by the fast Fourier transform (FFT) and taking the lowest significant frequency present in the spectrum. Tables 4.1 and 4.2 show a satisfactory agreement with the reference data from [7].

FIG. 3.3. *St. Venant-Kirchhoff: The deformation of the beam in case CSM3.*FIG. 3.4. *Neo-Hookean: The deformation of the beam in case CSM3.*

5. Interaction of compressible flow and elastic structures. The DGM described above is combined with the solution of compressible flow in a time dependent domain Ω_t and the resulting coupled problem is applied to the simulation of fluid-structure interaction. The boundary of Ω_t is formed by three disjoint parts: $\partial\Omega_t = \Gamma_I \cup \Gamma_O \cup \Gamma_{W_t}$, where Γ_I is the inlet, Γ_O is the outlet and Γ_{W_t} represents impermeable time-dependent walls.

The time dependence of the domain Ω_t is taken into account with the aid of the Arbitrary Lagrangian-Eulerian (ALE) method (see, e.g., [4] and [5]). It is based on a regular one-to-one ALE mapping of the reference configuration Ω_0 onto the current configuration $\Omega_t : \mathcal{A}_t : \bar{\Omega}_0 \rightarrow \bar{\Omega}_t$, i.e. $\mathbf{X} \in \bar{\Omega}_0 \mapsto \mathbf{x} = \mathbf{x}(\mathbf{X}, t) = \mathcal{A}_t(\mathbf{X}) \in \bar{\Omega}_t$. Further, we define the domain velocity $\tilde{\mathbf{z}}(\mathbf{X}, t) = \frac{\partial}{\partial t} \mathcal{A}_t(\mathbf{X})$, $t \in [0, T]$, $\mathbf{X} \in \bar{\Omega}_0$, $\mathbf{z}(\mathbf{x}, t) = \tilde{\mathbf{z}}(\mathcal{A}_t^{-1}(\mathbf{x}), t)$, $t \in [0, T]$, $\mathbf{x} \in \Omega_t$ and the ALE derivative of the state vector function $\mathbf{w} = \mathbf{w}(\mathbf{x}, t)$ defined for $\mathbf{x} \in \Omega_t$ and $t \in [0, T]$: $\frac{D^A}{Dt} \mathbf{w}(\mathbf{x}, t) = \frac{\partial \tilde{\mathbf{w}}}{\partial t}(\mathbf{X}, t)$, $\tilde{\mathbf{w}}(\mathbf{X}, t) = \mathbf{w}(\mathcal{A}_t(\mathbf{X}), t)$, $\mathbf{X} \in \bar{\Omega}_0$, $\mathbf{x} = \mathcal{A}_t(\mathbf{X})$. Then the continuity equation, the Navier-Stokes equations and the energy equation can be written in the ALE form

$$(5.1) \quad \frac{D^A \mathbf{w}}{Dt} + \sum_{s=1}^2 \frac{\partial g_s(\mathbf{w})}{\partial x_s} + \mathbf{w} \operatorname{div} \mathbf{z} = \sum_{s=1}^2 \frac{\partial R_s(\mathbf{w}, \nabla \mathbf{w})}{\partial x_s},$$

method	τ	$u_1 [\times 10^{-3}]$	$u_2 [\times 10^{-3}]$
ref		-14.305 ± 14.305 [1.0995]	-63.607 ± 65.160 [1.0995]
BDF2	0.04	-10.566 ± 9.963 [1.0675]	-64.866 ± 45.218 [1.0675]
BDF2	0.02	-13.477 ± 13.462 [1.0850]	-64.133 ± 61.177 [1.0850]
BDF2	0.01	-14.119 ± 14.111 [1.0900]	-63.905 ± 64.212 [1.0900]
BDF2	0.005	-14.454 ± 14.453 [1.0925]	-64.384 ± 64.939 [1.0925]

TABLE 4.1

CSM3: Comparison of the position of the point A for BDF2, St. Venant-Kirchhoff material and different time steps τ . The values are written in the format “mean value \pm amplitude [frequency]”.

p. degree	τ	$u_1 [\times 10^{-3}]$	$u_2 [\times 10^{-3}]$
ref		-14.305 ± 14.305 [1.0995]	-63.607 ± 65.160 [1.0995]
1	0.01	-14.119 ± 14.111 [1.0900]	-63.905 ± 64.212 [1.0900]
2	0.01	-14.159 ± 14.150 [1.0900]	-63.928 ± 64.290 [1.0900]
3	0.01	-14.061 ± 14.054 [1.0925]	-63.969 ± 64.246 [1.0925]

TABLE 4.2

CSM3: Comparison of the position of the point A for BDF2, St. Venant-Kirchhoff material and different polynomial degree of approximation in space. The values are written in the format “mean value \pm amplitude [frequency]”.

where $\mathbf{w} = (\rho, \rho v_1, \rho v_2, E)^T \in \mathbb{R}^4$, $\mathbf{g}_s(\mathbf{w}) = \mathbf{f}(\mathbf{w})_s - z_s \mathbf{w}$, $\mathbf{f}_s = (\rho v_s, \rho v_1 v_s + \delta_{1s} p, \rho v_2 v_s + \delta_{2s} p, (E+p)v_s)^T$, $\mathbf{R}_s(\mathbf{w}, \nabla \mathbf{w}) = (0, \sigma_{s1}^V, \sigma_{s2}^V, \sigma_{s1}^V v_1 + \sigma_{s2}^V v_2 + k \frac{\partial \theta}{\partial x_s})^T$, $s = 1, 2$, $\sigma_{ij}^V = \lambda \delta_{ij} \operatorname{div} \mathbf{v} + 2\mu d_{ij}(\mathbf{v})$, $d_{ij}(\mathbf{v}) = \frac{1}{2} \left(\frac{\partial v_i}{\partial x_j} + \frac{\partial v_j}{\partial x_i} \right)$, $i, j = 1, 2$. The following notation is used: ρ – fluid density, p – pressure, E – total energy, $\mathbf{v} = (v_1, v_2)$ – velocity vector, θ – absolute temperature, $c_v > 0$ – specific heat at constant volume, $\gamma > 1$ – Poisson adiabatic constant, $\mu > 0, \lambda = -2\mu/3$ – viscosity coefficients, $k > 0$ – heat conduction coefficient, σ_{ij}^V – components of the viscous part of the stress tensor. System (5.1) is completed by the thermodynamical relations $p = (\gamma - 1) \left(E - \rho \frac{|v|^2}{2} \right)$, $\theta = \frac{1}{c_v} \left(\frac{E}{\rho} - \frac{|v|^2}{2} \right)$ and equipped with the initial condition $\mathbf{w}(\mathbf{x}, 0) = \mathbf{w}^0(\mathbf{x})$, $\mathbf{x} \in \Omega_0$, and the boundary conditions:

$$\begin{aligned} \rho &= \rho_D, \quad \mathbf{v} = \mathbf{v}_D, \quad \sum_{j=1}^2 \left(\sum_{i=1}^2 \sigma_{ij}^V n_i \right) v_j + k \frac{\partial \theta}{\partial \mathbf{n}} = 0 \text{ on the inlet } \Gamma_I, \\ \mathbf{v} &= \mathbf{z}_D(t) = \text{velocity of a moving wall}, \quad \frac{\partial \theta}{\partial \mathbf{n}} = 0 \text{ on the moving wall } \Gamma_{W_t}, \\ \sum_{j=1}^2 \sigma_{ij}^V n_j &= 0, \quad \frac{\partial \theta}{\partial \mathbf{n}} = 0, \quad i = 1, 2, \text{ on the outlet } \Gamma_O, \end{aligned}$$

with prescribed data $\rho_D, \mathbf{v}_D, \mathbf{z}_D$. By \mathbf{n} we denote the unit outer normal.

The compressible flow problem is solved by the ALE space-time discontinuous Galerkin method described, e.g., in [1], [3].

In the FSI simulation we assume that the set $\Gamma_N^b \subset \Gamma_{W_0}$ and the common interface between the fluid and structure at time t is defined as $\tilde{\Gamma}_{W_t} = \{\mathbf{x} = \mathbf{X} + \mathbf{u}(\mathbf{X}, t); \mathbf{X} \in \Gamma_N^b\}$. The flow and structural problems are coupled by the transmission conditions

$$(5.2) \quad \mathbf{v}(\mathbf{x}, t) = \frac{\partial \mathbf{u}(\mathbf{X}, t)}{\partial t}, \quad \mathbf{P}(\mathbf{u}(\mathbf{X}, t)) \mathbf{n}(\mathbf{x}) = \boldsymbol{\sigma}^f(\mathbf{x}, t) \operatorname{Cof}(\mathbf{F}(\mathbf{u}(\mathbf{X}, t))) \mathbf{n}(\mathbf{x}),$$

$$\mathbf{X} \in \Gamma_N^b, \quad \mathbf{x} = \mathbf{X} + \mathbf{u}(\mathbf{X}, t), \quad \sigma_{ij}^f = -p \delta_{ij} + \sigma_{ij}^V.$$

We solve the FSI problem by a partitioned coupling mechanism, where the elasticity problem and the flow problem are solved separately. In order to satisfy the transmission conditions, we use a coupling procedure containing a few subiterations:

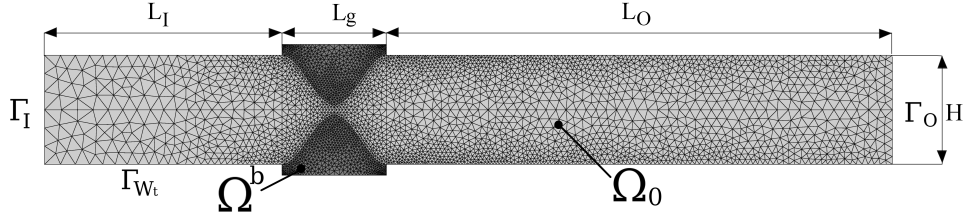


FIG. 5.1. Computational domain with the mesh at time $t = 0$ and the description of its size: $L_I = 50$ mm, $L_g = 15.4$ mm, $L_O = 94.6$ mm, $H = 16$ mm. The width of the channel in the narrowest part is 1.6 mm.

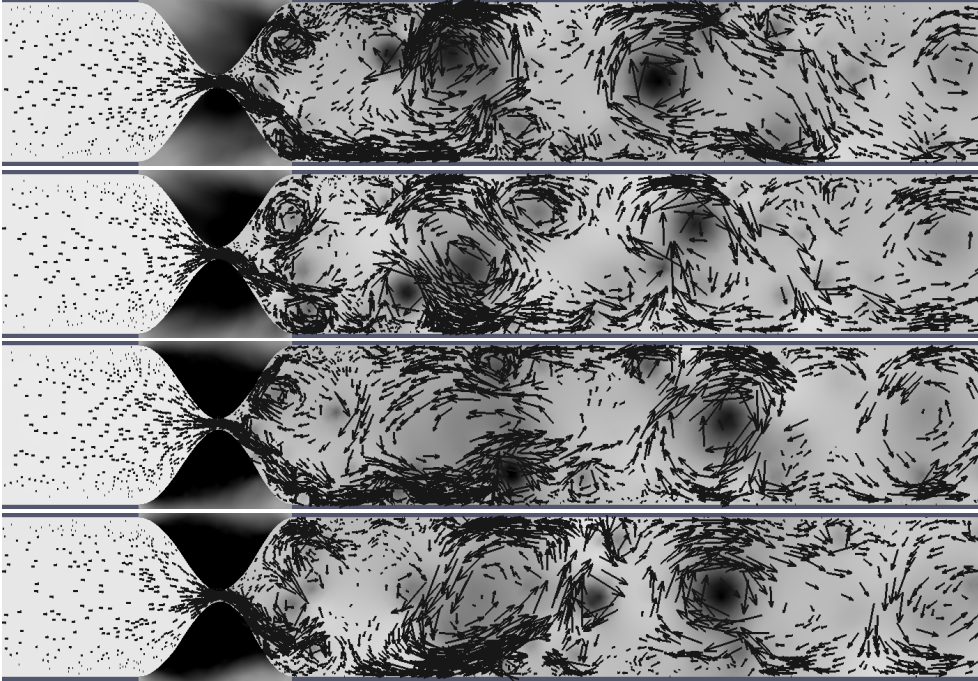


FIG. 5.2. Pressure and velocity distribution in the vocal tract at time instants $t = 0.0032, 0.0036, 0.004, 0.0044$ s.

1. Assume that the approximate solution $\mathbf{w}_{h\tau,k}$ of the flow problem in the time interval $[t_{k-1}, t_k]$ and the displacement of the structure $\mathbf{u}_{h,k}$ at the time level t_k are known.
2. We set $\mathbf{u}_{h,k+1}^0 := \mathbf{u}_{h,k}$, $l := 1$ and apply the following iterative process:
 - (a) Interpolate $\mathbf{u}_{h,k+1}^{l-1}$ on the common boundary of the fluid and the structure domain in order to get a continuous function on this interface.
 - (b) The approximation $\Omega_{t_{k+1}}^l$ of the domain $\Omega_{t_{k+1}}$ is determined by the interpolated displacement of the moving part of the fluid domain boundary.
 - (c) Determine the ALE mapping $\mathcal{A}_{t_{k+1}h}^l$ and approximate the domain velocity $\mathbf{z}_{h\tau,k+1}^l$.
 - (d) Solve the flow problem in the domain $\Omega_{t_{k+1}}^l$ to obtain the approximate solution $\mathbf{w}_{h\tau,k+1}^l$ in the time interval $[t_k, t_{k+1}]$.

- (e) Compute the stress tensor τ_{ij}^f and the aerodynamic force acting on the structure and transform it to the reference configuration Γ_N^b .
- (f) Solve the elasticity problem in order to compute the displacement $\mathbf{u}_{h,k+1}^l$ at time t_{k+1} .
- (g) If the variation $\left| \mathbf{u}_{h,k+1}^l - \mathbf{u}_{h,k+1}^{l-1} \right|$ of the displacement is larger than a prescribed tolerance, go to a) and set $l := l + 1$.
- (h) Set $\mathbf{u}_{h,k+1} := \mathbf{u}_{h,k+1}^l$, $\mathbf{w}_{h\tau,k+1} := \mathbf{w}_{h\tau,k+1}^l$ and $k := k + 1$ and go to 2.

The presented algorithm represents the so-called *strong coupling* scheme. Omitting (g) yields the so-called weak coupling scheme.

As an example of the FSI problem we present the simulation of vibrations of vocal folds, which are caused by the airflow originated in human lungs. We use a simplified geometry of vocal tract and vocal folds shown in Figure 5.1. Figure 5.2 shows the pressure distribution and the velocity field containing a number of vortices in the deformed vocal tract at time instants $t = 0.0032, 0.0036, 0.004, 0.0044$ s. The light shades correspond to higher pressure, whereas the dark shades represent low pressure. The pressure is in the range between 90950 and 98400 Pa = the inlet pressure, the outlet pressure is 97611 Pa. The inlet velocity is 4 ms^{-1} . The deformation of the vocal folds was computed with the use of St. Venant-Kirchhoff model. We see that the deformations of the vocal folds are very small. In this case the results are identical with those obtained by the linear elasticity model. The solution of situations with large deformations is in progress.

In the computation, the strong coupling had to be used. The stopping criterion was 10^{-6} , but only 3 iterations were necessary. In the first iteration, the maximal relative error in the displacement is $err = 0.028$. In the 2nd iteration we have $err = 0.000011$ and in the 3rd iteration $err = 2.02 \cdot 10^{-7}$.

Acknowledgments. This research was supported by the grants 13-00522S (M. Feistauer, M. Hadrava and A. Kosík) and P101/11/0207 (J. Horáček) of the Czech Science Foundation.

REFERENCES

- [1] J. ČEŠENEK, M. FEISTAUER AND A. KOSÍK, *DGFEM for the analysis of airfoil vibrations induced by compressible flow*, Z. Angew. Math. Mech., vol **93** (2013), No. 6-7, 387–402.
- [2] P. G. CIARLET, *Mathematical Elasticity, Volume I, Three-Dimensional Elasticity*, Volume 20 of Studies in Mathematics and its Applications, Elsevier Science Publishers B.V., Amsterdam, 1988.
- [3] V. DOLEJŠÍ AND M. FEISTAUER, *Discontinuous Galerkin Method, Analysis and Applications to Compressible Flow*, Volume 48 of Springer Series in Computational Mathematics, Springer, Cham, 2015.
- [4] M. FEISTAUER, J. HORÁČEK, V. KUČERA AND J. PROKOPOVÁ, *On numerical solution of compressible flow in time-dependent domains*, Mathematica Bohemica, **137** (2011), 1-16.
- [5] T. NOMURA AND T. J. R. HUGHES, *An arbitrary Lagrangian-Eulerian finite element method for interaction of flow and a rigid body*, Comput. Methods Appl. Mech. Engrg., **95** (1992), 115-138.
- [6] I.R. TITZE, *Principles of Voice Production*, National Centre for Voice and Speech, Iowa City, 2000.
- [7] S. TUREK, J. HRON, *Proposal for numerical benchmarking of fluidstructure interaction between an elastic object and laminar incompressible flow*, in: H. J. Bungartz, M. Schäfer (Eds.), Fluid-Structure Interaction: Modelling, Simulation, Optimisation, Springer, Berlin, 2006, 371-385.